Frequency-dependent polarizability of –CC– linked para-nitroaniline monomer through pentamer

Jeff Nichols [1] **and Jack Simons**

Chemistry Department, University of Utah, Salt Lake City, UT 84112, USA

Received 14 April 1993; in final form 25 May 1993

Using atomic orbital basis sets calibrated in an earlier study on the monomer and dimer and employing the direct atomic-integral driven strategy of the DISCO program package, we performed self-consistent field level calculations of the frequency-dependent polarizabilities of the monomer through pentamer of –CC– linked para-nitroaniline. These computations, which were performed in parallel using seven IBM RS6000 model 560 workstations, involved up to 612 atomic basis functions and 10^{11} two-electron integrals, and required solution of linear response equations whose dimensions ranged up to 132000.

1. Introduction

In an earlier work, we formulated and implemented a direct atomic-integral driven method for the calculation of frequency-dependent response properties at the self-consistent field (SCF) level [1]. By avoiding the two-electron integral transformation step and the need to store and retrieve the atomic-orbital (ao) based integrals, we were able to use large basis sets. The practicality of the approach was illustrated and calibrated by examining the scaling of the dipole polarizability (α) with the size of the system for para-nitroaniline (*p*NA) and its dimer. These calculations were carried out on an IBM 3090-600 supercomputer.

Except for a small positive enhancement of the polarizability component α_{zz} along the long molecular axis passing through the two nitrogen atoms, we found little effect of size on α for this system. However, when the –NN– linkage of the *p*NA dimer ($H_2NC_6H_4$–NN–$C_6H_4NO_2$) was replaced by a –CC– linkage, thus more effectively extending the π-orbital conjugation by making the molecule planar, we found a large frequency-dependent increase in the z component of the polarizability for the dimer relative to twice that of the monomer (factors varying from 3 to 18, depending on frequency). These observations make the –CC– linked polymer a potential candidate for achieving non-linear chain length dependence of properties that depend on α and provided the motivation to extend this study to longer chain lengths. In this Letter, we report the results of such extension, a task that involved carrying out calculations with 612 atomic orbitals and solving linear response equations of dimension 132000.

To make the evaluation of the frequency-dependent polarizability computationally feasible for larger chain lengths, we needed to migrate our methods and computer codes to a distributed processor environment. Recently, we were able to demonstrate the use of a cluster of workstations as an alternative supercomputing resource by combining a parallelized implementation of the same direct atomic-integral driven technology used in our earlier *p*NA work with various distributed computing interface tools (PVM, TCGMSG, Network Linda, and Parasoft Express) [2]. Using a cluster of eight IBM RISC System 6000 workstations (seven model 560s and one model 350), the distributed version of the ab initio direct SCF and random-phase approximation (RPA) code named DISCO [3], together with the PVM and TCGMSG message passing environments, we have now been able to reproduce the monomer and dimer calculations (run previously on the IBM 3090-600)

[1] Also with the Utah Supercomputing Institute and the IBM Federal Systems Company.

and to successfully extend the chain length to the pentamer.

Included in the calculations reported here are ab initio SCF-level geometry optimizations as well as static and frequency-dependent polarizability calculations (at five different frequencies) for each of these species. In section 2 we briefly review the pertinent aspects of the "direct" technology that we used with respect to SCF and RPA response calculations and our earlier basis set calibrations. In section 3, we discuss some of the computational challenges that arise, and in section 4 we display our results for the polarizability and analyze the frequency and chain-length dependence of these polymers.

2. Calculational methods

2.1. Brief overview of "direct" implementation

As detailed in ref. [1], the polarizability α at a frequency $\omega = 2\pi E/h$ can be written as

$$\alpha(E) = -2(r \quad -r)\begin{pmatrix} \mathbf{E}-\mathbf{A} & -\mathbf{B}^* \\ -\mathbf{B} & -\mathbf{E}-\mathbf{A}^* \end{pmatrix}^{-1}\begin{pmatrix} r \\ -r \end{pmatrix}. \quad (1)$$

In this expression,

(i) the virtual (m) to occupied (a) molecular orbital-level matrix elements $\{r_{ma} = \langle \phi_m | r | \phi_a \rangle\}$ of the three Cartesian components of the electric dipole operator are collected into the vector denoted r;

(ii) the elements of the $\mathbf{A}$ and $\mathbf{B}$ matrices, denoted $A_{ma;nb}$ and $B_{ma;nb}$, are given in terms of the orbital energies $\{\varepsilon_j\}$ and two-electron integrals:

$$A_{ma;nb} = \delta_{mn}\delta_{ba}(\varepsilon_m - \varepsilon_a) - (mn|ba) + 2(ma|bn), \quad (2a)$$

$$B_{ma;nb} = (an|bm) - 2(am|bn). \quad (2b)$$

Here Mulliken notation is used for the two-electron integrals:

$$(mn|ba) = \int \phi_m^*(1)\phi_n(1)|r_{12}^{-1}|\phi_b^*(2)\phi_a(2)\, d\tau_1\, d\tau_2, \quad (3)$$

and the indices m and n (a and b) are used to label virtual (occupied) SCF molecular orbitals.

In practice, the matrix inverse multiplied by vector product

$$\begin{pmatrix} \mathbf{E}-\mathbf{A} & -\mathbf{B}^* \\ -\mathbf{B} & -\mathbf{E}-\mathbf{A}^* \end{pmatrix}^{-1}\begin{pmatrix} r \\ -r \end{pmatrix}$$

appearing in the expression for $\alpha(E)$ is *not* computed by forming the inverse matrix explicitly; rather it is evaluated by employing iterative matrix-times-vector methods to solve the set of linear equations

$$\begin{pmatrix} \mathbf{E}-\mathbf{A} & -\mathbf{B}^* \\ -\mathbf{B} & -\mathbf{E}-\mathbf{A}^* \end{pmatrix}\begin{pmatrix} Z \\ Y \end{pmatrix} = \begin{pmatrix} r \\ -r \end{pmatrix}. \quad (4)$$

Once such an iterative process has converged and the $\binom{Z}{Y}$ solution vector is in hand, the polarizability is computed as

$$\alpha(E) = -2(r \quad -r)\begin{pmatrix} Z \\ Y \end{pmatrix}. \quad (5)$$

The key development in implementing the "direct" ao-driven approach introduced in ref. [1] is to reexpress all of the quantities involved in forming the matrix-times-vector products such as $\mathbf{A}Z$, $\mathbf{A}Y$, $\mathbf{B}Z$, and $\mathbf{B}Y$ in terms of ao rather than mo integrals; in this way, the DISCO program's loop structure can be used to distribute the (time consuming) calculation of groups of two-electron integrals over several processors. To derive the ao-driven expressions needed to compute such matrix-times-vector products, one first inserts the ao-to-mo integral transformation expression

$$(mn|ba) = \sum_{ijkl} C_{mi}C_{nj}C_{bk}C_{al}(ij|kl) \quad (6)$$

into each matrix–vector product to obtain, for example,

$$((\mathbf{E}-\mathbf{A})Z - \mathbf{B}Y)_{ma} = (\mathbf{E}-\varepsilon_m+\varepsilon_a)Z_{ma} + \sum_{nb}\sum_{ijkl} C_{im}C_{jn}C_{kb}C_{la} \times \{[(ij|kl) - 2(il|kj)]Z_{nb} + [2(li|kj) - (lj|ki)]Y_{nb}\}. \quad (7)$$

One next defines the (two-index transformed) ao-indexed Z_{jk} and Y_{jk} arrays as

$$\sum_{nb} C_{jn}C_{kb}Z_{nb} = Z_{jk}, \quad (8a)$$

$$\sum_{nb} C_{jn} C_{kb} Y_{nb} = Y_{jk} , \tag{8b}$$

as well as the following ao-indexed two-electron integral combinations:

$$A_{il,jk} = 2(il|kj) - (ij|kl) , \tag{9a}$$

$$B_{il,jk} = -2(li|kj) + (lj|ki) . \tag{9b}$$

These definitions allow the desired matrix–vector product to be written as

$$((\mathbf{E}-\mathbf{A})\mathbf{Z}-\mathbf{B}\mathbf{Y})_{ma} = (\mathbf{E}-\varepsilon_m+\varepsilon_a)Z_{ma} - \sum_{ijkl} C_{im} C_{la} \{A_{il,jk} Z_{jk} + B_{il,jk} Y_{jk}\} . \tag{10a}$$

The corresponding expression for the other matrix–vector product is:

$$(-\mathbf{B}\mathbf{Z}-(\mathbf{E}+\mathbf{A})\mathbf{Y})_{ma} = (-\mathbf{E}-\varepsilon_m+\varepsilon_a)Y_{ma} - \sum_{ijkl} C_{im} C_{la} \{B_{il,jk} Z_{jk} + A_{il,jk} Y_{jk}\} . \tag{10b}$$

The computer implementation in an ao-integral-driven manner then involves:

(1) using the mo-indexed, r_{ma}, Y_{ma} and Z_{ma} arrays from the preceding iteration of the linear equation solution process to form $Z_{jk} = \sum_{nb} C_{jn} C_{kb} Z_{nb}$, $Y_{jk} = \sum_{nb} C_{jn} C_{kb} Y_{nb}$, and $r_{jk} = \sum_{nb} C_{jn} C_{kb} r_{nb}$,

(2) using DISCO's integral generation power to compute and sum (it is in this step that the distributed processing occurs) contributions to the following two two-indexed arrays:

$$Q_{il} = \sum_{kj} \{B_{il,jk} Z_{jk} + A_{il,jk} Y_{jk}\}$$

and

$$P_{il} = \sum_{kj} \{A_{il,jk} Z_{jk} + B_{il,jk} Y_{jk}\} ,$$

(3) once the Q and P arrays are fully evaluated, they are (two-index) transformed to the ao basis to give $Q_{ma} = \sum_{il} C_{im} C_{la} Q_{il}$ and $P_{ma} = \sum_{il} C_{im} C_{la} P_{il}$.

This then allows the full right-hand sides of eqs. (10) to be compared. This is the rate limiting step in solving the linear response equations using the methods outlined in more detail in ref. [1].

2.2. Basis calibration on cyclopropenone and pNA monomer and dimer

The cyclopropenone (CP) molecule C_3H_2O was used in ref. [1] to develop an atomic orbital basis set for subsequent use on the target para-nitroaniline (*p*NA) molecule, its *N*-mers, and the –CC– linked analogs. CP was thought to be a reasonable "basis calibration" molecule because, like *p*NA, it contains a delocalized π-orbital network involving heteroatoms. However, because it contains only four "heavy" (i.e. non-hydrogen) atoms, it is possible to explore ao basis sets that are large enough to yield $\alpha(E)$ data accurate to within ±10% compared to the SCF limit (i.e. ignoring electron correlation effects). Such basis exploration was carried out in search of an ao basis capable of providing a ±10% level description of $\alpha(E)$ that is computationally feasible for use on the –CC– linked *p*NA pentamer.

In ref. [1], tests were also carried out with various atomic basis sets on the *p*NA monomer and its dimer. For the present purposes, suffice it to say that for each such *N*-mer, we first optimized the geometry using the analytical gradient routines contained in the DISCO package and an atomic orbital basis set [4] of [6, 3|3, 2] quality for non-hydrogen atoms and [3|2] quality for the hydrogen atoms. The resultant optimized geometry for the monomer (*p*NA) compares favorably to the excellent results found in ref. [5], and to experimental findings (ref. [5], and references therein). In particular, our structural parameters are all within 0.005 Å for bond distances and 0.8° for bond angles of those given in ref. [5]. The optimized geometries of the monomer through pentamer are available upon request. At such optimized geometries, all subsequent SCF and RPA calculations were performed with the atomic orbital basis set denoted 0P in ref. [1], which consists of van Duineveldt's [6, 3|4, 3] basis for non-hydrogen atoms and [3|3] for the hydrogen atoms.

3. Computational timings and mainframe-workstation cluster comparison

3.1. Scaling of computational effort with N

Having calibrated the ao bases as discussed above, we undertook the considerably more challenging task of calculating $\alpha(E)$ for the –CC– linked *p*NA *N*-mers ($N = 1, 2, ..., 5$) using the 0P basis.

Data pertinent to the computational complexity of

Table 1
Scaling of computational complexity with chain length N

Number of monomer units (N)	Number of atoms	Number of electrons	Number of ao basis functions (OP basis)	Number of two-electron integrals	Number of occupied orbitals	Number of un-occupied orbitals	Dimension of A and B arrays
1	16	72	148	4.8×10^{8}	36	112	4032
2	28	124	264	4.9×10^{9}	62	202	12524
3	40	176	380	2.1×10^{10}	88	292	25696
4	52	228	496	6.1×10^{10}	114	382	43548
5	64	280	612	1.4×10^{11}	140	472	66080

the SCF and RPA calculations are summarized in table 1. Of particular note are:

(i) that the number of two-electron integrals that need to be computed (each taking, on average ≈ 500 floating point operations) grows to ≈ 140 billion, which would require ≈ 280 Gby of disk space *if* these integrals were to be stored, and

(ii) that the combined dimensions of the A and B arrays entering into the linear equations solved to compute $\alpha(E)$ ranges up to ≈ 132000.

The number of two-electron integrals (column 5) scales as the number of ao basis functions (column 4) to the fourth power. These integrals must be recalculated for each iteration of the SCF and RPA polarizability calculation. Each such iteration will also require either solution of a matrix eigenvalue problem (i.e. the SCF orbital energy eigenvalue problem whose dimension equals the size of the basis set) or solution of a set of linear equations (with dimension equal to the combined dimensions of the A and B matrices (i.e. twice column 8)). The SCF and RPA polarizability calculations usually converge in fewer than 30 iterations.

3.2. Workstation cluster timings for $N=1, 2, ..., 5$

In carrying out the calculations whose timings are reported below in table 2, we used a master–slave distributed computing approach (using the PVM and TCGMSG messaging passing tools) on a cluster of seven workstations, with one RISC System 6000 560 as the master and six 560s as slaves. The slaves were used to compute the ao-based two-electron integral and to accumulate contributions to the SCF Fock matrix (which was subsequently diagonalized by the master) or to the RPA linear equation matrix (then solved by the master). The resulting wall times (roughly equal to the CPU times) per iteration of the SCF eigenvalue calculation or of the RPA polarizability linear equation solution are given in table 2.

Table 2
Wall times (in minutes per iteration) for SCF eigenvalue and RPA polarizability linear equation solutions on a seven station cluster

Number of –CC– linked *p*NA monomers	SCF eigenvalue solution	Polarizability linear equation solution
1	0.5	1.3
2	2.5	8.3
3	7.5	22.5
4	16.5	47.3
5	32	83.5

3.3. Comparison to IBM 3090-600 timings

Table 3 provides a timing comparison for the cluster and our earlier results obtained on the IBM 3090-600 for the monomer and dimer. One can immediately see why we were able to extend our calculations to include the pentamer on the workstation cluster when less than a year ago this calculation on the 3090 would not have been tenable.

4. Results

The –CC– linked *p*NA N-mer results obtained in this study of $\alpha(E)$ for selected frequencies $h\omega/2\pi=E$

Table 3
Timings [a] for the –CC– linked *p*NA monomer and dimer on the seven workstation cluster and on one processor of an IBM 3090-600

Number of monomer units	Frequency ω in atomic units	Wall time on IBM 3090-600	Wall time on the workstation cluster
1	0.0 (static)	1.4	0.2
1	0.028838	3.0	0.4
1	0.164713	4.0	0.6
2	0.0 (static)	10.6	1.2
2	0.028838	29.7	3.0
2	0.164713	48.1	6.2

[a] Time (in h) to compute the polarizability at frequency ω; a converged solution of the linear equations is required.

are displayed in table 4; the frequencies (reported in eV) chosen are identical to those used in ref. [1]. The x, y, and z axes are: the z-axis is the "long axis" of each N-mer; the y-axis lies perpendicular to the symmetry plane of the molecule; and the x-axis lies in the symmetry plane of the molecule.

Our calculated monomer (*p*NA) properties include a dipole moment of $\mu = 2.901$ au, a long-axis polarizability component of $\alpha_{zz} = 121.3$ au^3, and one third the trace of $\alpha = 83$ au^3. These data can be compared to the calculated results found in ref. [5] where $\mu = 3.154$ au and $\alpha_{zz} = 140.3$ au^3 (at the HF level of theory) and to experiment [6] which gives $\mu = 2.479$ au and $\alpha = 148.5$ au^3.

One of the most striking features of this data is the difference between the N dependence of α_{zz} and those of α_{xx} and α_{yy}. Clearly, α_{xx} and α_{yy} vary less than linearly with N; a least squares fit of α_{xx} and α_{yy} versus N to a quadratic function of N gives negative values for their N^2 dependence: $\alpha_{xx} \approx 19 + 72N - 0.33N^2$ and $\alpha_{yy} \approx 3.4 + 34N - 0.14N^2$ at $\omega = 0$, and $\alpha_{xx} \approx 22 + 93N - 1.25N^2$ and $\alpha_{yy} \approx 4.5 + 35N - 0.0N^2$ at the highest frequency $\omega = 4.48$ eV. In contrast, α_{zz} displays higher than linear scaling, which is one of the primary findings of this work; a least squares fit of the $\omega = 4.48$ eV data gives: $\alpha_{zz} \approx -138 + 246N + 28N^2$; for the static polarizability, the fit produces $\alpha_{zz} \approx -90 + 199N + 9N^2$. The important point is that the quadratic term is negative (and small) for α_{xx} and α_{yy} but it is positive (and much larger) for α_{zz}.

In fig. 1 we illustrate the N dependence of α_{zz} for zero frequency (i.e. the static polarizability case) and

Table 4
Frequency dependent polarizability α (au^3), energy E (hartree), and dipole moment μ (au) for –CC– linked *p*NA monomer through pentamer

Frequency ω (eV)	Monomer $E = -486.750247$ au $\mu = 2.90$ au			Dimer $E = -790.547688$ au $\mu = 3.435$ au			Trimer $E = -1094.349441$ au $\mu = 3.600$ au			Tetramer $E = -1398.152337$ au $\mu = 3.663$ au			Pentamer $E = -1701.955139$ au $\mu = 3.690$ au		
	α_{xx}	α_{yy}	α_{zz}	α_{xx}	α_{yy}	α_{zz}	α_{xx}	α_{yy}	α_{zz}	α_{xx}	α_{yy}	α_{zz}	α_{xx}	α_{yy}	α_{zz}
0.00	90.7	37.0	121.3	162.0	69.9	337.9	232.0	102.8	590.2	301.7	135.6	857.4	371.2	168.4	1130.8
0.65	91.1	37.1	122.5	162.8	70.1	342.9	233.1	103.0	600.8	303.1	135.9	874.6	373.0	168.8	1154.9
2.10	94.1	37.5	130.4	168.1	71.0	380.8	240.6	104.3	684.2	312.8	137.6	1011.9	384.7	170.9	1350.3
2.99	98.1	38.1	142.8	175.4	72.1	451.6	250.8	105.9	855.2	325.9	139.8	1310.6	400.7	173.6	1792.2
4.09	107.3	39.3	182.6	192.4	74.2	896.9	274.4	109.0	2912.6	355.8	143.8	9288.5	436.9	178.6	56371.3
4.48	112.6	39.9	219.7	202.7	75.3	3987.6	288.4	110.6	−2657.0	373.3	145.9	−1997.6	457.8	181.1	−1952.6

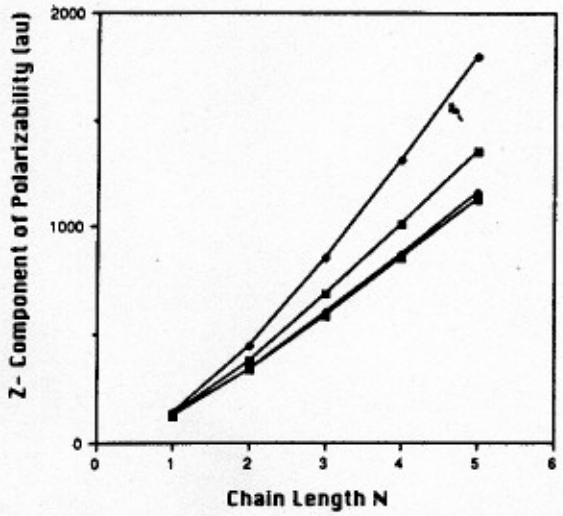

Fig. 1. Plots of the z component of polarizability (in au^3) for –CC– linked pNA N-mers versus N; frequencies are in eV. (⊡) $\omega=0$, (♦) $\omega=0.65$, (■) $\omega=2.10$, (◇) $\omega=2.99$.

for three frequencies lying below the first electronic excitation energy. At a transition frequency, $\alpha(E)$ displays a singularity and moves from $+\infty$ to $-\infty$. There is a clear non-linearity in the N dependence of α_{zz}. Not only does α_{zz} scale with chain length in a manner that depends on frequency, but the quadratic dependence on N is more pronounced at higher frequency.

The physical reason for the qualitative difference between the N dependences of α_{xx}, α_{yy}, and α_{zz} becomes clear when one relates these components of α to the dipole moments that are induced if an electric field of strength E were applied along the x, y, or z axes:

$$\mu_z=\alpha_{zz}E, \quad \mu_x=\alpha_{xx}E, \quad \mu_y=\alpha_{yy}E\,.$$

The delocalized nature of the π-orbital network allows electron density to be readily polarized along the z axis, whereas the more localized σ and π bonding along the (in plane) x axis and the even more localized bonding along the (perpendicular to the plane) y axis do not permit such a large degree of electron density polarization. Moreover, as the chain length N grows, the distance over which orbitals are delocalized along the z axis grows, but the extent of delocalization along the y and x axes remains fixed. Finally, as N grows, the HOMO–LUMO energy gap is reduced, thus causing α to grow. It is for these reasons that α_{zz} grows more strongly with N than α_{xx} and α_{yy}.

Acknowledgement

This work was supported by the Office of Naval Research and by the National Science Foundation, Grant No. CHE9116286. We wish to thank the Utah Supercomputing Institute for staff and computer resources. In particular we wish to thank USI for early access and several weeks of dedicated time on the newly acquired cluster of RISC System 6000 workstations.

References

[1] M. Feyereisen, J. Nichols, J. Oddershede and J. Simons, J. Chem. Phys. 96 (1992) 2978.
[2] M. Feyereisen, R. Kendall, J. Nichols, D. Dame and J. Golab, An implementation of the direct SCF and RPA methods on loosely coupled networks of workstations, J. Comput. Chem., accepted for publication (May 1993), and references therein.
[3] J. Almlöf, K. Fægri Jr., M. Feyereisen and K. Korsell, DISCO, a direct SCF and MP2 code.
[4] F.B. van Duijneveldt, IBM Res. RJ 945 (1971).
[5] F. Sim, S. Chin, M. Dupuis and J. Rice, J. Phys. Chem. 97 (1993) 1158.
[6] A. McClellan, Tables of experimental dipole moments (Rahara, El Cerrito, CA, 1974);
L. Cheng, W. Tam, S. Stevenson and G. Meredith, J. Phys. Chem. 95 (1991) 10631.